IC/87/222
INTERNAL REPORT
(Limited distribution)

International Atomic Energy Agency
and
United Nations Educational Scientific and Cultural Organization

INTERNATIONAL CENTRE FOR THEORETICAL PHYSICS

ARTIFICIAL NOISE DUE TO DC ELECTRIC TRAINS *

W.E. Senanayake
International Centre for Theoretical Physics, Trieste, Italy.

ABSTRACT

The current distribution in a DC railway and the resulting magnetic effects have been modelled using the parameters of the DC railway networks in Italy. The results show that the magnetic perturbations are substantially high in the vicinity of electrified railway lines. The order of magnitude of the induced field can be as significant as $\sim 40nT$ at a distance of $\simeq 2km$ from the railway line indicating that geophysical techniques that employ natural magnetic anomalies can be badly effected, within this range. The magnetic effects rapidly decay with increasing distance, but the noise level could be significant even at a range $\sim 10km$. Also, these induced anomalies vary significantly with the conductivity of the ground. When the conductivity is high it is possible that the railway currents dispersed through the ground interact with those induced in the earth, causing a severe disruption to the telluric measurements.

MIRAMARE - TRIESTE
August 1987

* Submitted for publication.

1 Introduction

The electromagnetic induction studies of the earth often encounter with the problem of artificial noise of different character. For instance, it has been observed that the electromagnetic field measurements are quite sensitive to the coast effects (Weaver, 1965; Podney, 1975; Dosso et. al.,1986), and to the seismic disturbances (Breiner, 1964; Kahalas, 1965). The types of disturbances commonly found in the field recordings, however, are mainly due to electric power networks (e.g. high tension power lines, industrial plants, domestic electrical goods etc.). Since AC power generators are used in most cases, it may be possible, at least, to minimize the associated noise arising at the frequency of $50\ Hz$ and its harmonics, by introducing some form of filtering system (e.g. Simon and Rossignol, 1974; Adams et. al.,1986). However, the problem will become more complicated if the network concerned is that of a high tension DC power supply. In this case, the perturbations may not be filtered out, because the DC effects usually cover a wide frequency range. Although DC power networks are not common, one clear example of their presence is that the DC electrified railway networks like those found in Italy. Therefore, a study of the possible disturbances caused by these circuits would be useful for gaining insight into the nature of the DC noise problem.

Linington (1974 *a*) has investigated the noise problem associated with the DC electric trains in Italy.But the illustration of the possible effects, given in his paper, is restricted to the level of static measurements (magnetic and archeology prospecting). Moreover, the approach made by Linington (1974 *a*) with regard to the current distribution in the railway network needs improvements, because it neglects the effects of the return currents through the running rails.

The present paper analyses the magnetic effects due to DC electric trains, with a view to demonstrating the type of noise in relation to geophysical methods that employ natural magnetic anomalies of both static and transient character. It is attempted here to model the magnitude as well as the time dependence of the induced magnetic perturbations. The circuit parameters used in the present model are those of the Italian Railways, obtained from the Italian Railway Department. It will not be that difficult to demonstrate (see section 3) that the magnitude and the direc-

tion of the DC railway currents vary as trains move along the railway track. But, to determine these time dependent DC currents to a high accuracy will be more difficult because certain variables related to the network tend to change circumstantially.

2 DC Railway Network in Italy

Since a detailed description of the general characteristics of the Italian railways is available elsewhere (Musso, 1954; Linington, 1974 *a*; Buffarini and Rosa, 1976), only the important points about the voltage and current supply are summarized here.

The DC power supplied into the railway network is actually generated by the rectification of a high tension AC supply ($\simeq 132\,kV$) at the railway sub-stations located in quite regular intervals along the railway line. The average distance between two sub-stations is $20\,km$, but it could vary from $15 - 40\ km$ depending upon the traffic density and the topography of the railway line. The magnitude of the DC voltages used in Italy also varies from $\simeq 800\,V$ from urban railways to $\simeq 3600\,V$ for national (long distance) railways. Since the geophysical measurements are usually made in areas quite far away from big cities, a nominal voltage of $3500\,V$ may be more appropriate for the present considerations.

The railway current circuit, except in special areas like railway stations and junctions, can be considered as a series of sections, each being bounded by two successive sub-stations (Fig. 1 *a*). For a train within a certain section, the current supply to the train engine (locomotive) comes through the overhead wires (contenary) connected between the two neighbouring sub-stations. These currents vary depending upon the position of the train, even if the total power drawn by the locomotive and hence the total current remains constant. As far as the railway circuit is concerned, there will be no current flow between any two adjacent sub-stations in absence of trains moving in that section. If there are other trains on the adjacent sections of the line as well, then the current distribution in the particular section concerned will be altered due to additional current outputs coming from the other sub-stations.

The efficiency of a locomotive is $\sim 6 - 8\ MW$ and hence is capable of drawing currents up to $\sim 2500\ A$. At every sub-station there exists a system of automatic switching to regulate the maximum current through the contenary and to protect the railway circuit from short-circuiting and over-loading (Buffarini and Rosa, 1976). A train travelling under normal conditions (i.e. when the motion is undisturbed) will maintain a nearly constant speed $\simeq 140\,km\,h^{-1}$, drawing current $\sim 1500 - 2000\,A$. But, these currents fluctuate quite rapidly as the motion of the train is subject to irregularities (e.g. at stations & junctions and during acceleration, climbing hills etc.).

The current entering into the rails through the weels of the locomotive will return to the sub-stations partly along the two steel rails running parallel and partly through the ground. One cannot neglect the proportion of return currents dispersed through the ground, in spite of the fact that the rails are placed on horizontal wooden bars fixed on the dry gravel of very low conductivity. The reason why the currents through the ground become significant is that, in practice, the rails are short-circuited and grounded at every $1\ km$ or so along the track as a protective measure (Fig. 1 *a*). The resistance/unit length of a steel rail varies from $0.08\,\Omega\,km^{-1}$ to $0.06\,\Omega\,km^{-1}$ as the area of cross section varies from $320\,mm^2$ to $440\,mm^2$.

3 The Current Distribution

One should consider both the overhead currents and return currents, in describing the current distribution in the railway circuit. But, as already mentioned, the dependence of the railway currents on a number of factors causes some difficulty in trying to determine them at a high accuracy. Therefore, it is necessary to introduce a model to reduce the practical situation to a less complicated situation, so that a reasonable estimation of the current distribution is possible. Essentially, this approach needs making a few assumptions about certain variables related to the railway network. The assumptions made here are as follows;

(*a*). the railway line is almost straight (*b*). the topographic effects on the line are insignificant (*c*). the traffc input on the line at a given situation is represented by a single train travelling at nearly a constant speed, and (*d*). the sub-stations are situated at regular distances.

As can be seen from Figs. 1 *a* & 1 *b*, the situation for a train travelling between any two sub-stations S_{n-1} and S_n ($n = 1, 2, 3, \ldots$) may be approximated, to an equivalent battery circuit.

For the battery circuit having voltage parameters E, r_i & V (Fig. 1 *b*);

$$E - V = I_1(r_i + \rho l) = I_2[r_i + \rho(L - l)] \tag{1}$$

where I_1 & I_2 are the instantaneous currents drawn from the sub-stations S_{n-1} & S_n respectively as the train is positioned at a distance l from S_{n-1}, L is the distance between the two sub-stations, and $\rho = \rho_1 + \rho_2$; ρ_1 & ρ_2 are the resistance/unit length of the contenary and of the railway track respectively.

As indicated above, the locomotive is supplied with a balance current for a train travelling under normal conditions, and so;

$$\begin{aligned} I_1 + I_2 &= I \simeq constant \\ \frac{I_1}{I_2} &\simeq \frac{L - l}{l} \end{aligned} \tag{2}$$

Based on the above assumptions, Fig. 1 *c* gives the current distribution between the two supply wires for the situation of Fig. 1 *a*. In all cases, the currents from left to right are considered as positive.

The presentation of the return currents is more difficult because a significant proportion of these currents tends to flow through the upper layers of the Earth. This proportion will much depend on the resistance of the steel rails, conductivity of the ground and the contact between the rails and the ground (see Appendix *A*). In order to clarify this point, the distribution of the return currents along the steel rails, as expressed in equation (13), is given schematically in Fig. 1 *d*.

Since the rails are grounded at regular intervals, the effective conductivity and hence the attenuation constant will be modified, accordingly as;

$$g' \sim g + \frac{n}{r_g L} \quad \text{and} \quad k = \sqrt{g'\rho_2}$$

where n is the number of grounded networks between two sub-stations, r_g is the average resistance of a grounded network and g is the conductivity of the ground.

Substituting typical values for, $L = 20\ km$, $n = 21$, $r_g = 0.6\ \Omega$, $\rho_2 = 0.06\ \Omega\, km^{-1}$ and $I = 1000\ A$, and considering that the conductivity, $g \sim 10^{-3} - 10^{-1}\ S\, m^{-1}$, the distributions of return currents corresponding to three different positions ($l = 4\ km$, $10\ km$, $16\ km$) between $S_{n-1}S_n$ are illustrated in Fig. 2. It is clearly demonstrated that the proportion of currents flowing through the ground varies significantly with the conductivity and also with changing distances between the train and the sub-stations.

The currents through the rails for a given value of l vary from one point to the other along the railway line as a function of x, because of the dispersion of currents through the ground at intermediate points (Fig. 2). Therefore, it is convenient to present the instantaneous currents along the rails in the form $< i >= {}_l\int i\, dx$, as averaged values over the distance along the line. From equation (13);

$$\begin{aligned} < i_1 > &= -\frac{I}{2kl}(1 - e^{-kl})\left[2 - \frac{l}{L}(1 + e^{-k(L-l)})\right] \\ < i_2 > &= \frac{I}{2k(L-l)}(1 - e^{-k(L-l)})\left[2 - \frac{L-l}{L}(1 + e^{-kl})\right] \\ < i_a > &= 0;\ < i_b >= 0 \end{aligned} \tag{3}$$

Therefore, the unbalanced currents flowing in the section $S_{n-1}S_n$ are;

$$\begin{aligned} \overline{I}_1 &= I_1 + < i_1 > \\ \overline{I}_2 &= I_2 + < i_2 > \end{aligned} \tag{4}$$

Using the values given above, it can be shown that $\overline{I}_1$ and $\overline{I}_2$ significantly vary according to the position of the train and reach a maximum near the sub-stations (Fig. 3).

4 The Magnetic Effects

In estimating the induced magnetic field perturbations, it is important that the situation of possible interest in relation to the railway network complies with the current distribution model given in the previous section. Accordingly, we shall set out the following conditions to describe the situation concerned here (also see Fig. 4);

(a). at time $t = 0$, a train travelling at a constant speed v_o passes point O, nearest position to the railway line from the point of observation P;

(b). at time t, the train is positioned at point T between two sub-stations S_{n-1} and S_n $(n = 1, 2, 3, ..)$, so that $OT = v_o t$,

(c). the current flow in each of the portions $S_{n-1}T$ & S_nT within section $S_{n-1}S_n$ is attributed to three straight conductors; one (contenary) at a distance p vertically above the other two (steel rails) running at a separation q.

Since $p \sim 4\ m$ and $q \sim 1\ m$ are negligibly small comparing with other distances considered, the current flow as given in case (c) may be reduced to a single straight conductor carrying an unbalanced current. Therefore the currents in the portions $S_{n-1}T$ and S_nT within section $S_{n-1}S_n$ may be represented by $\overline{I}_1$ & $\overline{I}_2$, as expressed in equation (4), respectively.

According to equation (17) in Appendix B, the magnetic field components at point P due to electric currents in $S_{n-1}T$ & S_nT are given respectively by;

$$\vec{B}_1 = \frac{\mu_o \overline{I}_1}{4\pi r_o^2} \left\{ \frac{v_o t}{\sqrt{r_o^2 + (v_o t)^2}} - \frac{d_{n-1}}{\sqrt{r_o^2 + d_{n-1}^2}} \right\} (-x_o \vec{k} + z_o \vec{i}) \qquad (5)$$

$$\vec{B}_2 = \frac{\mu_o \overline{I}_2}{4\pi r_o^2} \left\{ \frac{d_n}{\sqrt{r_o^2 + d_n^2}} - \frac{v_o t}{\sqrt{r_o^2 + (v_o t)^2}} \right\} (x_o \vec{k} - z_o \vec{i}) \qquad (6)$$

where $r_o = OP = \sqrt{x_o^2 + z_o^2}$ is the nearest distance between P and the train, and $d_n = nL - d_o$ is the distance to the n^{th} sub-station from O. So, the net effect,

$$\vec{B}_p = \vec{B}_1 + \vec{B}_2 = Cf(r_o, t) z_o \vec{i} - Cf(r_o, t) x_o \vec{k} \qquad (7)$$

where,

$$f(r_o, t) = \overline{I}_1 \left(\frac{v_o t}{\sqrt{r_o^2 + (v_o t)^2}} - \frac{d_{n-1}}{\sqrt{r_o^2 + d_{n-1}^2}} \right) - \overline{I}_2 \left(\frac{d_n}{\sqrt{r_o^2 + d_n^2}} - \frac{v_o t}{\sqrt{r_o^2 + (v_o t)^2}} \right)$$

and $C = \mu_o/(4\pi r_o^2)$, so that;

$$|\vec{B}_p| = \frac{\mu_o f(r_o, t)}{4\pi r_o^2} \qquad (8)$$

From the above expressions it can be seen immediatly that the net magnetic effect observed at P depends upon the position of the train and the distance to P from the train. However, in order to gain an even clearer idea about the field variation at P, a few samples of $|\vec{B}_p|$ corresponding to a number of different cases may by illustrated, using appropriate numerical values for various parameters.

Figs. 5, 6 & 7 give 3 sets of plots of $|\vec{B}_p|$ vs. l (or t), relative position of train (or relative time), for 3 different initial values, $d_o = 0, -6$ & $-12\,km$. Only the section S_oS_1, which is the nearest to P is considered in this case (i.e. when the situation specified above satisfies $n = 1$). Each set consists of four plots corresponding to $r_o = 0.1, 2, 10, 30\,km$, for 3 different values of the conductivity, g ranging from $\sim 10^{-3} - 10^{-1}\ S\,m^{-1}$. The speed of the train, v_o is considered to be $2\ km/min$. It is clearly demonstrated that the response at P varies considerably with the conductivity and the initial conditions, though the dependence on the latter becomes less acute at larger distances.

The variation of $|\vec{B}_p|$ plotted in semi-logarithmic scale (Fig. 8 *a*) for eight different values of r_o varying from $0.6 - 30\ km$, indicate that the magnitude of the magnetic disturbances in the vicinity of railway line is $\sim 1000\ nT$ and reduce substantially at longer distances ($\sim 10^{-2}\ nT$ as $r_o \sim 30\ km$). For convenience, only a single set of values for g and d_o are considered here,so that $g = 10^{-2}\ Sm^{-1}$ and $d_o = 0\ km$. The rapid decay of the perturbation with increasing r_o is further demonstrated in Fig. 8 *b*, which gives the instantaneous values of $|\vec{B}_p|$ against r_o in semi-logarithmic scale, as the train approaching a position at $6\,km$ away form O. This curve follows $\sim 1/r_o$ variation (dotted line curve) for $\leq 3\ km$, but the variation becomes more abrupt at larger distances.

If the railway line is oriented at an angle β, measured in clockwise direction, to the North,

$$\vec{B}_p = Cf(r_o, t) z_o \sin\beta\, \vec{n} + Cf(r_o, t) z_o \cos\beta\, \vec{e} + Cf(r_o, t) x_o \vec{k'} \qquad (9)$$

where $\vec{n}$, $\vec{e}$ and $\vec{k'}$ are the unit vectors along the north, east and vertically downwards directions. Unlike $|\vec{B}_p|$, the relative magnitudes of H, D and Z,

the components along the north-south, east-west and vertically downwards directions respectively, depend upon the vertical gradient z_o, which is the difference in level between the railway and P, and the orientation of the track.

From equations (5 - 9), the variation of the magnetic components at different points of observation can be computed. Table 1 gives the instantaneous values of H, D & Z anomalies at $t = 0$ (the time at which the train passes the nearest position to P), taking $g = 10^{-2}\ Sm^{-1}$, $\beta = 30^{o}$ and the values of the other parameters as before. For each of the seven values of r_o chosen here (i.e. $r_{oi}, i = 1, 2, ...7$), four different vertical gradients, given by $z^b_{oi}/r_{oi} = 0.25k$, $k = 0, 1, 2, 3$, are considered. It is sufficient to consider only this case for obtaining the order of magnitude of each component, because the values given in Table 1 are likely to represent the upper limit. These values indicate how effective the magnetic anomaly could be, when the point of observation is nearer to the railway line. It can also be seen that the anomalies get altered by quite large amounts when the vertical gradient is changed. But this effect gradually disappears with increasing r_o.

Only the section S_oS_1, which is the nearest, has so far been taken into consideration. Since the model used here is supposed to represent a general case, the above calculations may be extended to the neighbouring sections as well (i.e. $n \geq 1$).Accordingly, the variation of the Z component between sub-stations S_o & S_4, taking $n = 4$, is shown for a few selected values of r_o & z_o (Fig. 9). At distances $\leq 2\ km$ or so, the effects almost disappear (Fig. 9 *a* & 9 *b*) as the train leaves the nearest section, because the magnetic fields induced by the currents in the two portions $S_{n-1}T$ & S_nT, $n > 1$, are mutually cancelled out. As the distance becomes larger, the relative magnitude of effects arising at 2^{nd} and 3^{rd} section of the line may not be insignificant (Figs. 9 *c* & 9 *d*).

5 Discussion

The current distribution in a *DC* railway network and the possible magnetic effects associated with it have been analysed in the previous sections. As shown above, the rate of motion of the trains is the factor of prime importance concerning the railway noise problem, because it determines the current distribution in various sections of the circuit and hence the induced magnetic anomalies. The variation of the currents and the magnetic anomalies has been modeled, taking into consideration of the movement of a single train under normal conditions. However, it should be noted here that the above treatment provides only a general guide as the practical situation concerning the railway network is more complex than the situation considered in the present paper. The major obstacle involved here may be understood as being due to circumstantial changes that occurred in a railway circuit (e.g. currents, speed of the trains, conductivity of ground etc.), causing some degree of difficulty in determining the rate of variation of these parameters from one place to the other. Therefore, it becomes necessary to introduce some form of simplification to overcome this problem. Thus a number of assumptions is made in the present model in order to present the situation of possible interest in such a way that a reasonable estimate of the magnetic perturbations is possible. The factors which could considerably affect the situation considered in the model, in comparison with the practical situation, are;

(i) abrupt change in magnitude and direction of currents at the substations, (ii) current fluctuations near railway stations and junctions, and due to sudden changes in train speed, (iii) curvature and the topography of the railway line (iv) irregular traffic density on the line, and (v) dispersion of currents through the sorrounding layers of the earth.

In fact, the assumptions made in the model along with the complications pertaining to the railway circuit would undermine to a certain extent the accuracy of the estimated values. For instance, the theoretical curves for the variation of magnetic perturbations are quite smooth in contrast to those would have been obtained experimentally. The sudden changes of the

motion of train and the current fluctuations near sub-stations and junctions could cause impulses or jumps on the curves giving irregular shaped figures. Yet, the order of the effects as seen from the present calculations (see Table 1) is comparable with those observed in the vicinity of DC railway lines in Italy (e.g. Linington, 1974 b). Moreover, the graphical representation of the magnitude and the time dependence of the magnetic anomalies (Figs. 5 - 9) adequately resemble the character of noise due to a DC source, showing that the response at a given point could be effective over a wide range of frequencies. It is also demonstrated how the contribution to noise depend upon the rate of motion of the electric trains and the other parameters of the circuit and how the noise level varies with the distances from the railway line. The conductivity g ranging from $10^{-3} - 10^{-1}\, S\, m^{-1}$, the distance r_o varying from $100m$ to $30km$ and the DC currents $\sim 1000A$ used here suppose to resemble the typical values corresponding to the practical situation.

The magnetic perturbations as estimated from the model show that the DC trains could cause serious disturbances to both magnetic prospecting methods involving static field anomalies and electromagnetic induction studies (Magnetotelluric & Deep Magnetic Sounding) using transient magnetic variations of inospheric origin. The magnitude of the perturbation could be as strong as $\sim 40\, nT$ at a distance $\simeq 2\, km$ from the railway track. This suggests that any geophysical experiment based on magnetic anomalies may not be possible within this range. At a distance $\simeq 5\, km$ the effect reduces down to $\leq 8\, nT$. Even at this range, the noise level will be significant, particularly in relation to the natural elctromagnetic signals. A range of $\sim 10\, km$ seems to be quite safe for magnetic prospecting methods, though the signal to noise ratio could still be significant for natural signals.

It is quite possible that the AC electrified trains also present a source of noise. But the advantage concerning this type of noise is that it can be easily identified and hence the effects can be removed satisfactorily (Adams et. al., 1986). Unfortunately, this is not the case regarding the DC noise, as it represents a wide range of frequencies. Therefore, precautions should

be made in carrying out geophysical measurements in presence of a DC network, like the electric trains in Italy.

The railway effects become insignificant only at distances far away from the line ($r_o \geq 30\, km$). Therefore it is important that one avoids, whenever possible, the areas within a range of $\leq 25 - 30\, km$ from a DC railway line in selecting a site for induction measurements. The range of possible railway effects for prospecting methods will be shorter than the above case. Even if the nearest distance to an electrified railway line is sufficiently large, it is preferable to carry out measurements in quiet hours, when the traffic input on the track is minimum. This perhaps explains why the magnetotelluric measurements from many parts of Italy give unreliable results, as has been noted by a number of workers.

The possible effects arising from the currents dispersed through the ground have so far been ignored. In fact, these currents form another current distribution in the ground which presents an additional source of time dependent magnetic effect. It requires the solution of Laplace's equation in the ground to deal with this problem, and this will be discussed in a separate paper. In general, the contribution of these currents to the magnetic effects at a given point will be quite small, because the effective current density is much less than that due to currents in the conductors (rails & contenary). But if the conductivity of the ground is sufficiently high, these magnetic effects will also become significant. Moreover, it is possible that the dispersed currents cause disturbances to the telluric recordings. Since the distance between a train and sub-stations vary up to $\sim 20\, km$, the effects on the telluric measurements could be significant even at distances $r_o \sim 10\, km$ from the track. However, much will depend again on the conductivity of the sorrounding area and the distance at which the observations are made. Therefore, the MTS technique appears to be most sensitive to the noise coming from the DC electrified trains.

ACKNOWLEDGEMENTS

The author would like to thank the Ing. Mazzini of the Direzione del Compartimento di Bologna delle Ferrovie dello Stato for clarifying discussions, and the Italian Railway Department for providing the parameters of the Italian railway network used in the present study. Prof. A. H. Cook is gratefully acknowledged for his valuable comments. He would also like to thank Professor Abdus Salam, the International Atomic Energy Agency and UNESCO for hospitality at the International Centre for Theoretical Physics, Trieste.

APPENDIX A

The current, i and the contact voltage, v for a conductor of resistance/unit length, ρ which touches the ground may be expressed as;

$$\frac{di}{dx} = -gv$$
$$\frac{dv}{dx} = -\rho i \qquad (10)$$

where g is the average conductivity of the Earth's surface layers in contact with the conductor. The solution of this equation;

$$v = A_1 e^{kx} + A_2 e^{-kx}$$
$$i = \frac{1}{R_c}(A_2 e^{-kx} - A_1 e^{kx}) \qquad (11)$$

where $k = \sqrt{\rho g}$ is the attenuation constant, $R_c = \rho/k = \sqrt{\rho/g}$ is the characteristic resistance and A_1 & A_2 are the integration constants.

When a potential is applied between C & A and C & B of a conductor, so that $AB = L$ and $AC = l$ (Fig. 10 a), the distribution of current and voltage along the conductor as given by equation (11) is;

$$\begin{aligned}
v_1 &= A_1 e^{kx} + A_2 e^{-kx} \\
i_1 &= \frac{1}{R_c}(A_2 e^{-kx} - A_1 e^{kx}) && \text{for } 0 \le x \le l; \\
v_2 &= A_3 e^{kx} + A_4 e^{-kx} \\
i_2 &= \frac{1}{R_c}(A_4 e^{-kx} - A_3 e^{kx}) && \text{for } l \le x \le L; \\
v_a &= A_5 e^{kx} \\
i_a &= -\frac{1}{R_c} A_5 e^{kx} && \text{for } x \le 0; \\
v_b &= A_6 e^{-kx} \\
i_b &= \frac{1}{R_c} A_6 e^{-kx} && \text{for } x \ge L; \qquad (12)
\end{aligned}$$

Applying boundary conditions at A,B and C, the coefficients $A_1, A_2, \ldots, A_6$ can be determined as;

$A_1 = (R_c/2)(Ie^{-kl} - I_2 e^{-kl})$; $\quad A_2 = -(R_c/2)I_1$;

$A_3 = -(R_c/2)I_2 e^{-kL}$; $\quad A_4 = (R_c/2)(Ie^{-kl} - I_2 e^{-kL})$;

$A_5 = (R_c/2)(Ie^{-kl} - I_2 e^{-kL} - I_1)$ and

$A_6 = (R_c/2)(Ie^{kl} - I_1 - I_2 e^{kL})$

Substituting these values into equation (12);

$$
\begin{aligned}
v_1 &= \frac{R_c}{2}\left[-I_1 e^{-kx} + I e^{-k(l-x)} - I_2 e^{-k(L-x)}\right] \\
i_1 &= \frac{1}{2}\left[-I_1 e^{-kx} - I e^{-k(l-x)} + I_2 e^{-k(L-x)}\right] \qquad \text{for } 0 \le x \le l; \\
v_2 &= \frac{R_c}{2}\left[-I_1 e^{-kx} + I e^{-k(x-l)} - I_2 e^{-k(L-x)}\right] \\
i_2 &= \frac{1}{2}\left[-I_1 e^{-kx} + I e^{-k(x-l)} + I_2 e^{-k(L-x)}\right] \qquad \text{for } l \le x \le L; \\
v_a &= \frac{R_c}{2}\left[-I_1 e^{kx} + I e^{-k(l-x)} - I_2 e^{-k(L-x)}\right] \\
i_a &= \frac{1}{2}\left[I_1 e^{kx} - I e^{-k(l-x)} + I_2 e^{-k(L-x)}\right] \qquad \text{for } x \le 0; \\
v_b &= \frac{R_c}{2}\left[-I_1 e^{-kx} + I e^{-k(x-l)} - I_2 e^{-k(x-l)}\right] \\
i_b &= \frac{1}{2}\left[-I_1 e^{-kx} + I e^{-k(x-l)} - I_2 e^{-k(x-L)}\right] \qquad \text{for } x \ge L; \qquad (13)
\end{aligned}
$$

APPENDIX B

The magnetic flux density due to an element $d\vec{l}$ of current I at a point P specified by the vector $\vec{r}$ is given by the Biot-Savart law, as;

$$d\vec{B} = \frac{\mu_o I(d\vec{l} \wedge \vec{r})}{4\pi|\vec{r}|^3} \qquad (14)$$

where the permeability of free space $\mu_o = 4\pi \times 10^{-7} Hm^{-1}$.

According to equation (14), the magnetic field at point $P(x_o, z_o)$ due to a straight current wire oriented along the Y axis (Fig. 10.b) may be expressed as;

$$
\begin{aligned}
\vec{B} &= \frac{\mu_o I}{4\pi}\int_l \frac{d\vec{l} \wedge \vec{r}}{|\vec{r}|^3} \\
\vec{B} &= \frac{\mu_o I}{4\pi}(\vec{j} \wedge \vec{r_o})\int_l \frac{dl}{|\vec{r}|^3} \qquad (15)
\end{aligned}
$$

where $\vec{r_o} = x_o\vec{i} + z_o\vec{k}$ and $\vec{i}$, $\vec{j}$ & $\vec{k}$ are the unit vectors along X, Y & Z axes respectively.

Substituting $|\vec{r}| = r_o \sec\theta$ and $dl = r_o \sec^2\theta d\theta$, where $r_o = |\vec{r_o}| = \sqrt{x_o^2 + z_o^2}$, into equation (15);

$$\vec{B} = \frac{\mu_o I}{4\pi}(\vec{j} \wedge \vec{r_o})\int_{\alpha_1}^{\alpha_2} \frac{d\theta}{r_o^2 \sec\theta} \qquad (16)$$

where α_1 and α_2 are the angles made by the two edges of the wire at P and now,

$$\vec{B} = \frac{\mu_o I}{4\pi r_o^2}(\sin\alpha_2 - \sin\alpha_1)(-x\vec{k} + z\vec{i}) \qquad (17)$$

REFERENCES

Adam, A., Szarka, L., Vero, J. and Wallner, A., Magnetotelluric (MT) in mountains - noise, topographic and crustal inhomogeneity effects, Phys. Earth Planet. Int., 42, 165-177, 1986.

Buffarini, G.G. and Rosa, S.L., Miglioramento nella protezione dai corto-circuiti sulle linee di contatto F.S. 3 kV C.C. (Internal publications, Italian Railways) 1976.

Breiner, S., Piezomagnetic effect at the time of local earthquakes, Nature, 202, 790- 91, 1964.

Dosso, H.W., Chan, G.H. and Nienaber, W., An analogue model study of EM induction for an island near and cape coastlines, Phys. Earth Planet. Int., 42, 178-183, 1986.

Fraser, S.L., Excitation of extremely low frequency electromagnetic waves in the earth inosphere by high altitude nuclear detonations', J.Geophys. Res., 70, 3587-3594, 1965.

Hennington, R.E., The magnetic disturbances caused by DC electric railways, Prospezioni Archeologiche, 9, 9 - 20, 1974 a.

Hennington, R.E., Magnetic electrical and coring surveys at Colle del Forno, Monteliberti- 1970-1973', Prospezioni Archeologiche, 9, 47-59, 1974 b.

Musso, G., Natura Fisica della difesa dalla corrosione per elettrolisi', Ingegneria Ferroviaria, 5, 367-375, 1954.

Podney, W., Electromagnetic field genereated by Ocean waves, J. Geophys. Res., 80, 2977-2990, 1975.

Simon, G. and Rossignol, J.C., A recording system for the earth's telluric field with either analog or numerical output, Phys. Earth. Planet. Int., 8, 19-22, 1974.

Weaver, J.T., Magnetic variation associated with ocean waves and swell', J. Geophys. Res., 70, 1921-1929, 1965.

TABLE 1: Instantaneous values of the components of the induced magnetic field.

r (km)	z (km)	H(nT)	D(nT)	Z(nT)	$\lvert B_p \rvert$ (nT)
0.1	0.000	0.000	0.000	1010.149	1010.149
	0.025	126.269	218.704	978.073	1010.149
	0.050	252.538	437.407	874.815	1010.149
	0.075	378.807	656.111	668.150	1010.149
0.5	0.000	0.000	0.000	185.752	185.752
	0.063	11.610	20.108	184.295	185.752
	0.125	23.219	40.216	179.853	185.752
	0.188	34.828	60.325	172.196	185.752
1.0	0.000	0.000	0.000	77.542	77.542
	0.083	3.231	5.596	77.273	77.542
	0.167	6.462	11.192	76.458	77.542
	0.250	9.693	16.788	75.080	77.542
2.0	0.000	0.000	0.000	27.605	27.605
	0.125	0.863	1.494	27.551	27.605
	0.250	1.725	2.988	27.388	27.605
	0.375	2.588	4.482	27.115	27.605
5.0	0.000	0.000	0.000	5.501	5.501
	0.250	0.138	0.238	5.494	5.501
	0.500	0.275	0.476	5.473	5.501
	0.750	0.413	0.715	5.439	5.501
10.0	0.000	0.000	0.000	1.064	1.064
	0.417	0.022	0.038	1.063	1.064
	0.833	0.044	0.077	1.060	1.064
	1.250	0.067	0.115	1.056	1.064
30.0	0.000	0.000	0.000	0.015	0.015
	1.071	0.000	0.000	0.015	0.015
	2.143	0.001	0.001	0.015	0.015
	3.214	0.001	0.001	0.015	0.015

FIGURE CAPTIONS:

Fig. 1 : (a) A section of the railway network bounded by two successive sub-stations (b) an equivalent battery circuit (c) currents along the contenary and (d) currents through the rails.

Fig. 2 : The distribution of return currents for (a) ℓ = 4 km (b) ℓ = 10 km ,and (c) ℓ = 16 km.

Fig. 3 : The current distribution in the railway network.

Fig. 4 : Schemetic representation of the situation of possible interest as considered in the text.

Fig. 5 : Variation of the induced magnetic effect at P with ℓ , when S coincides with point P (i.e d_o= 0 km), for (a) r_o= 0.1 km (b) r_o = 2 km (c) r_o = 10 km and (d) r_o= 30 km.

Fig. 6 : Variation of the magneti effects when d_o= -6 km.

Fig. 7 : Variation of the magnetic effects when d_o= -12 km.

Fig. 8 (a) & (b) : Dependence of the induced magnetic effects on the value of r_o.

Fig. 9 : Variation of the Z component of the magnetic disturbance with ℓ.

Fig. 10: Illustration of the (a) dispersion of current through the ground and (b) Magnetic effects due to a straight current wire.

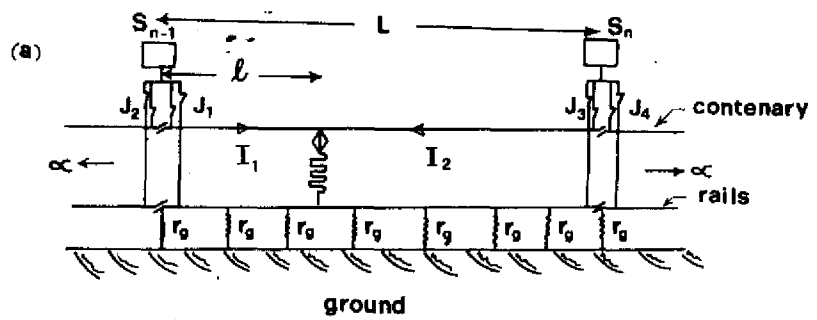

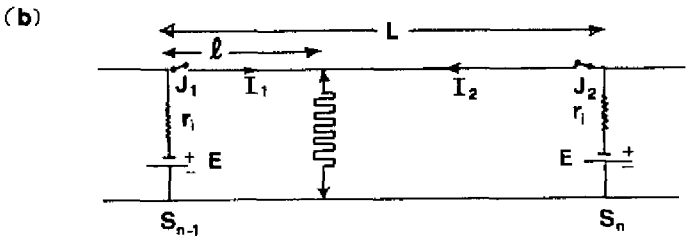

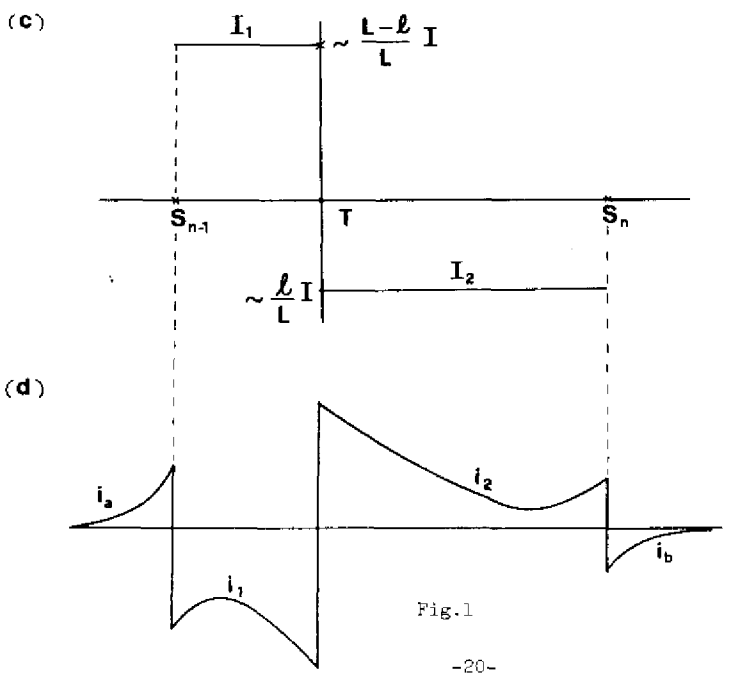

Fig.1

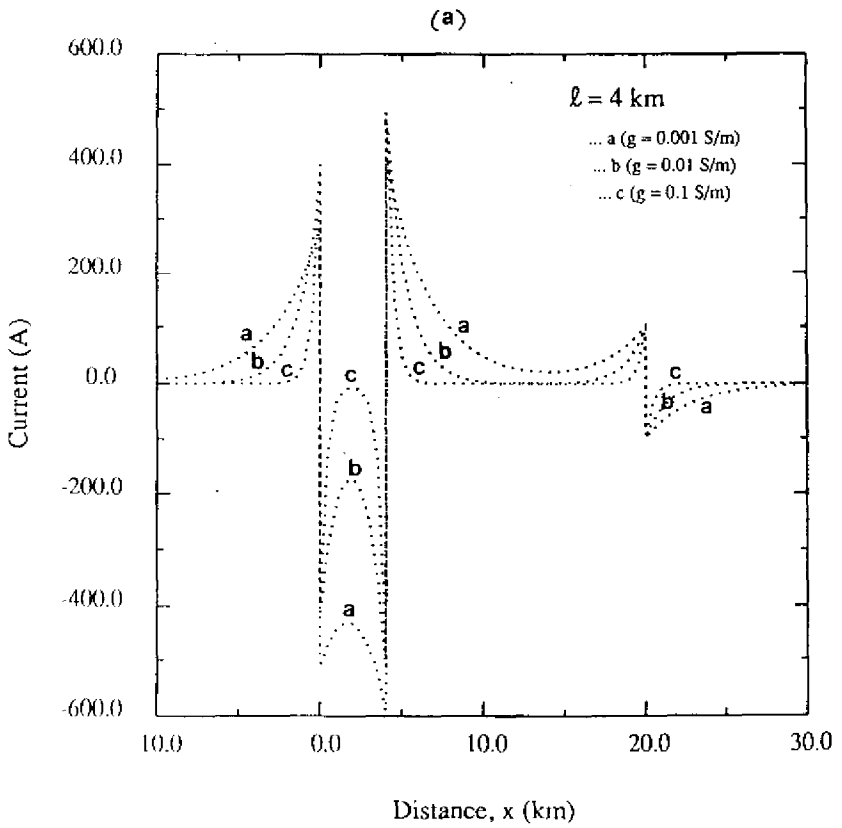
(a)
ℓ = 4 km
... a (g = 0.001 S/m)
... b (g = 0.01 S/m)
... c (g = 0.1 S/m)
Current (A)
600.0
400.0
200.0
0.0
-200.0
-400.0
-600.0
10.0
0.0
10.0
20.0
30.0
Distance, x (km)

Fig. 2a

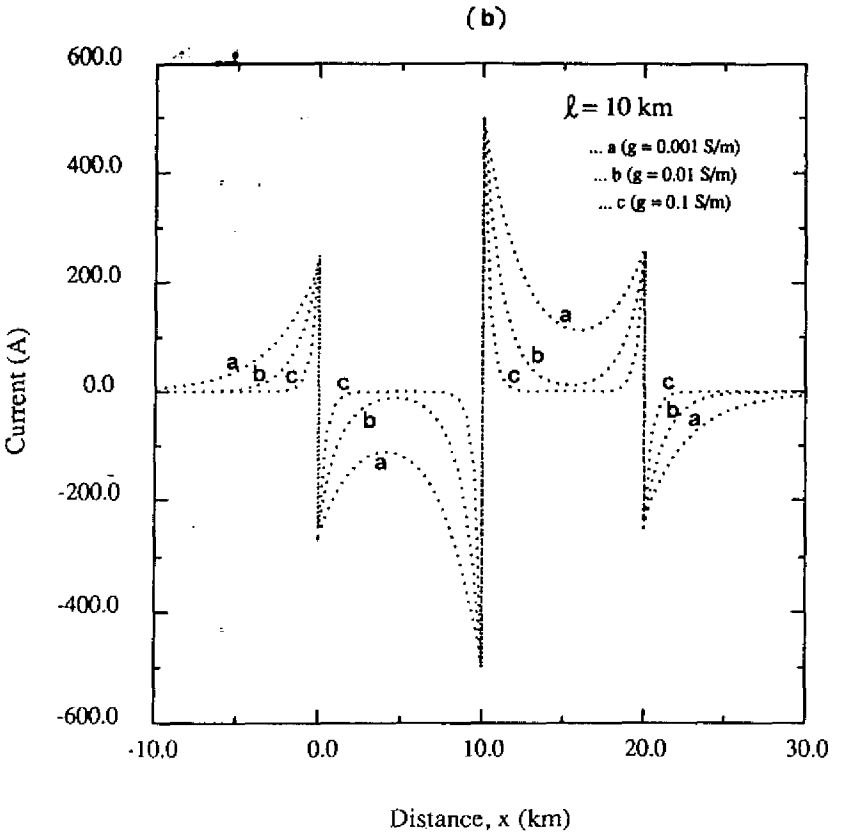
(b)
ℓ = 10 km
... a (g = 0.001 S/m)
... b (g = 0.01 S/m)
... c (g = 0.1 S/m)
Current (A)
600.0
400.0
200.0
0.0
-200.0
-400.0
-600.0
-10.0
0.0
10.0
20.0
30.0
Distance, x (km)

Fig. 2b

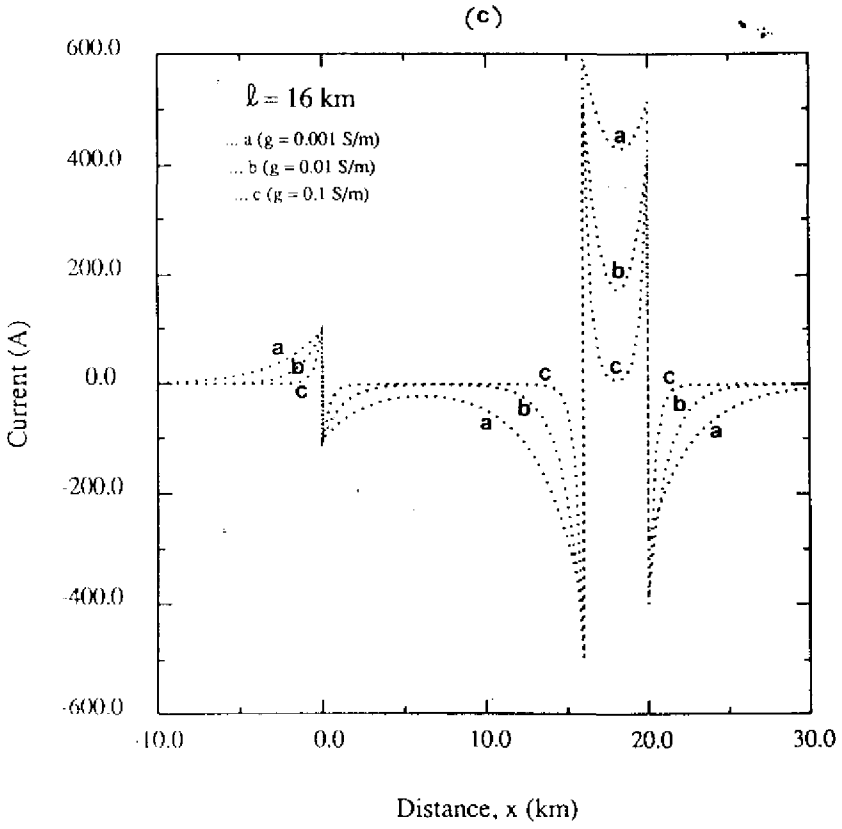
(c)
ℓ = 16 km
... a (g = 0.001 S/m)
... b (g = 0.01 S/m)
... c (g = 0.1 S/m)
600.0
400.0
200.0
0.0
-200.0
-400.0
-600.0
-10.0
0.0
10.0
20.0
30.0
Current (A)
Distance, x (km)

Fig.3c

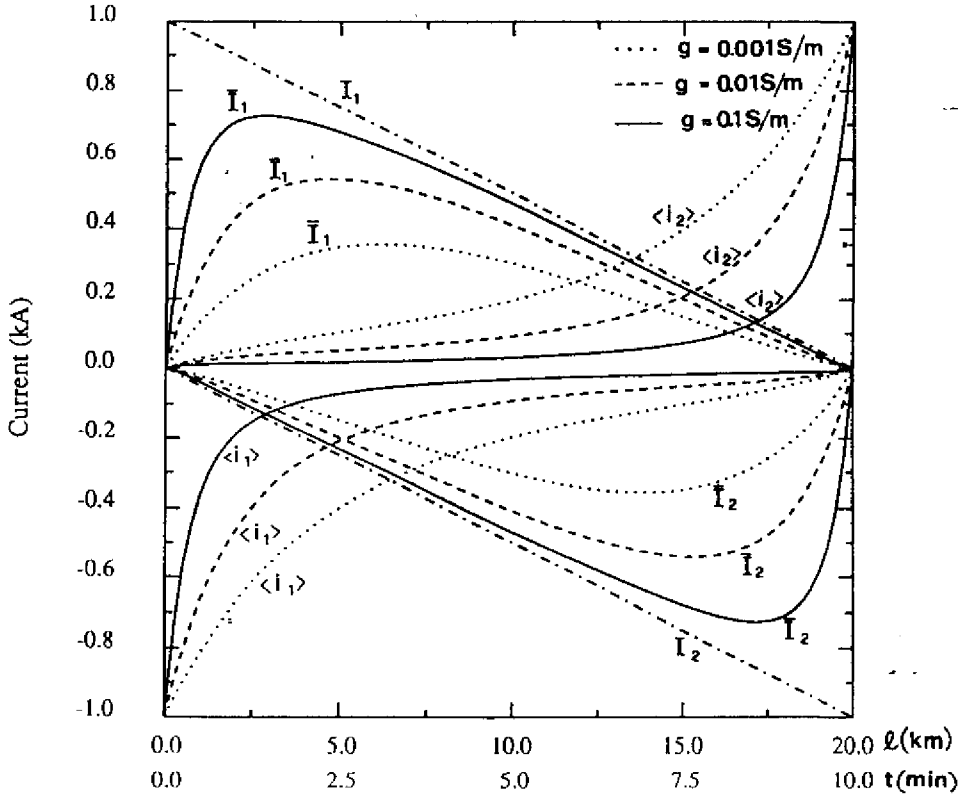
g = 0.001S/m
g = 0.01S/m
g = 0.1S/m
1.0
0.8
0.6
0.4
0.2
0.0
-0.2
-0.4
-0.6
-0.8
-1.0
Current (kA)
0.0
5.0
10.0
15.0
20.0 ℓ(km)
0.0
2.5
5.0
7.5
10.0 t(min)

Fig.3

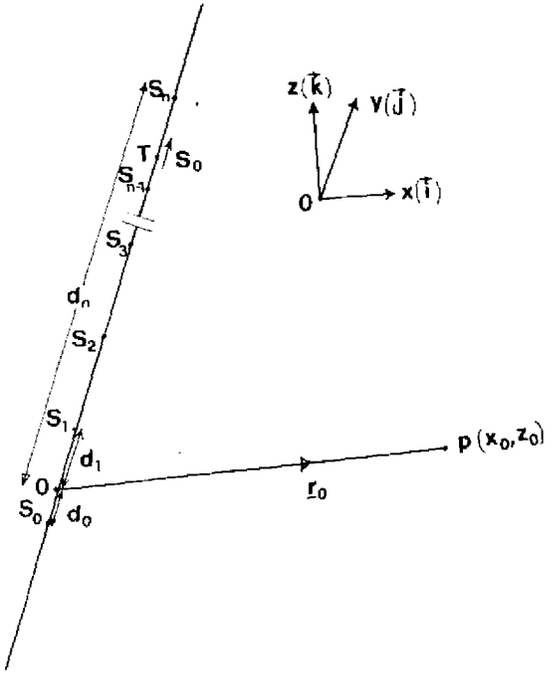
S_n
T
S_0
S_{n-1}
S_3
d_n
S_2
S_1
d_1
0
S_0
d_0
z(k)
y(j)
0
x(i)
p (x_0, z_0)
r_0

Fig. 4

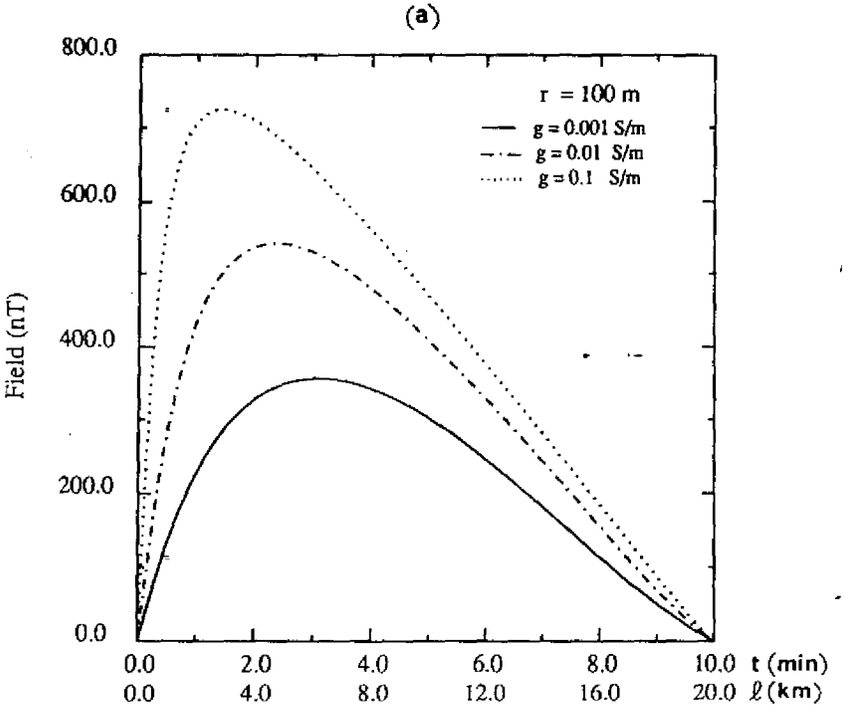
(a)
800.0
600.0
400.0
200.0
0.0
Field (nT)
r = 100 m
g = 0.001 S/m
g = 0.01 S/m
g = 0.1 S/m
0.0
2.0
4.0
6.0
8.0
10.0 t (min)
0.0
4.0
8.0
12.0
16.0
20.0 ℓ (km)

Fig. 5a

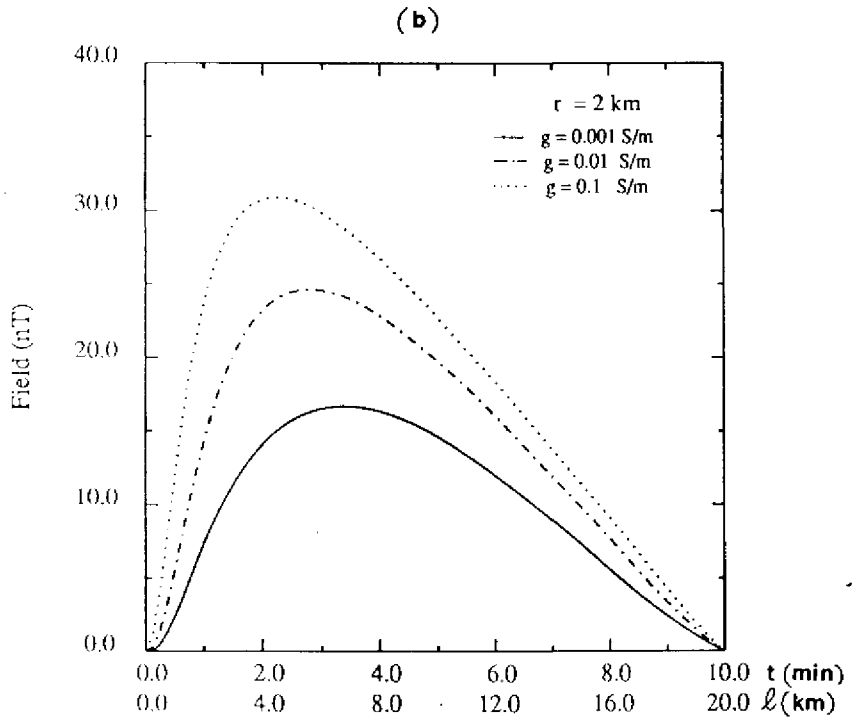
(b)
r = 2 km
g = 0.001 S/m
g = 0.01 S/m
g = 0.1 S/m
Field (nT)
40.0
30.0
20.0
10.0
0.0
0.0 2.0 4.0 6.0 8.0 10.0 t (min)
0.0 4.0 8.0 12.0 16.0 20.0 ℓ (km)

Fig. 5b

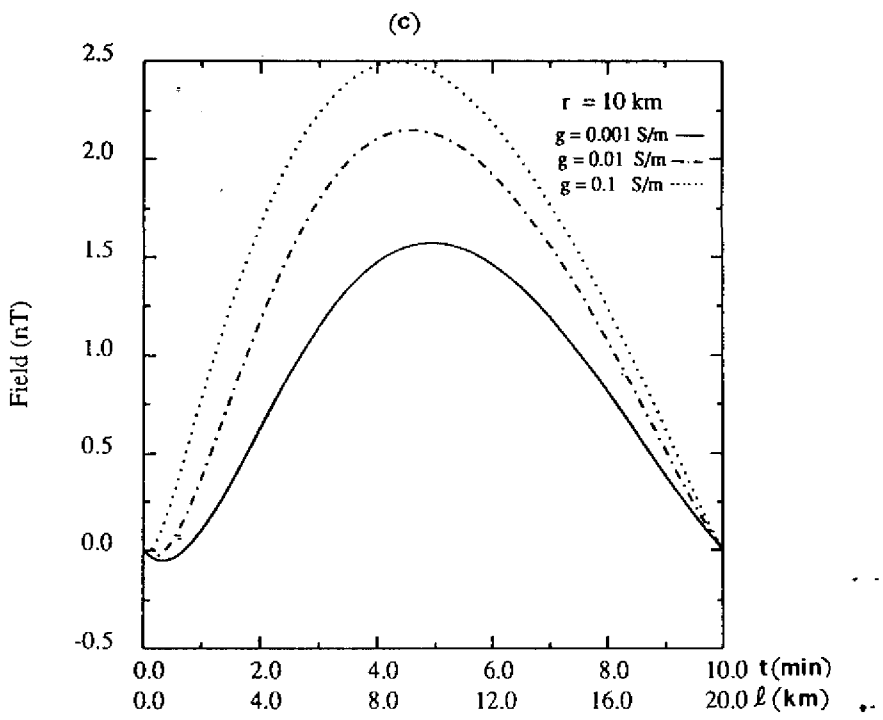
(c)
r = 10 km
g = 0.001 S/m
g = 0.01 S/m
g = 0.1 S/m
Field (nT)
2.5
2.0
1.5
1.0
0.5
0.0
-0.5
0.0 2.0 4.0 6.0 8.0 10.0 t(min)
0.0 4.0 8.0 12.0 16.0 20.0 ℓ (km)

Fig. 5c

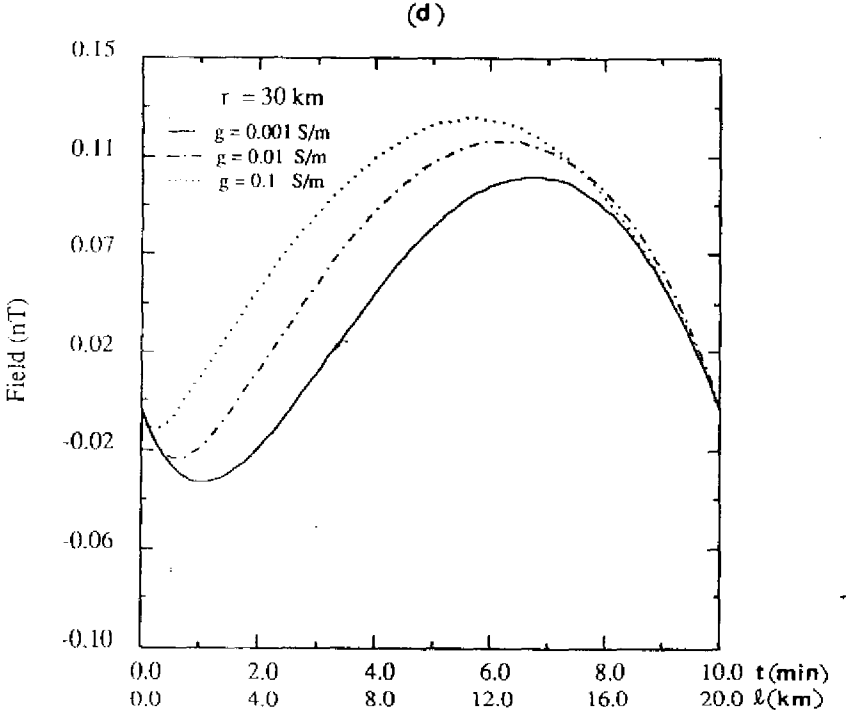
(d)
r = 30 km
g = 0.001 S/m
g = 0.01 S/m
g = 0.1 S/m
Field (nT)
0.15
0.11
0.07
0.02
-0.02
-0.06
-0.10
0.0
2.0
4.0
6.0
8.0
10.0 t(min)
0.0
4.0
8.0
12.0
16.0
20.0 ℓ(km)

Fig. 5d

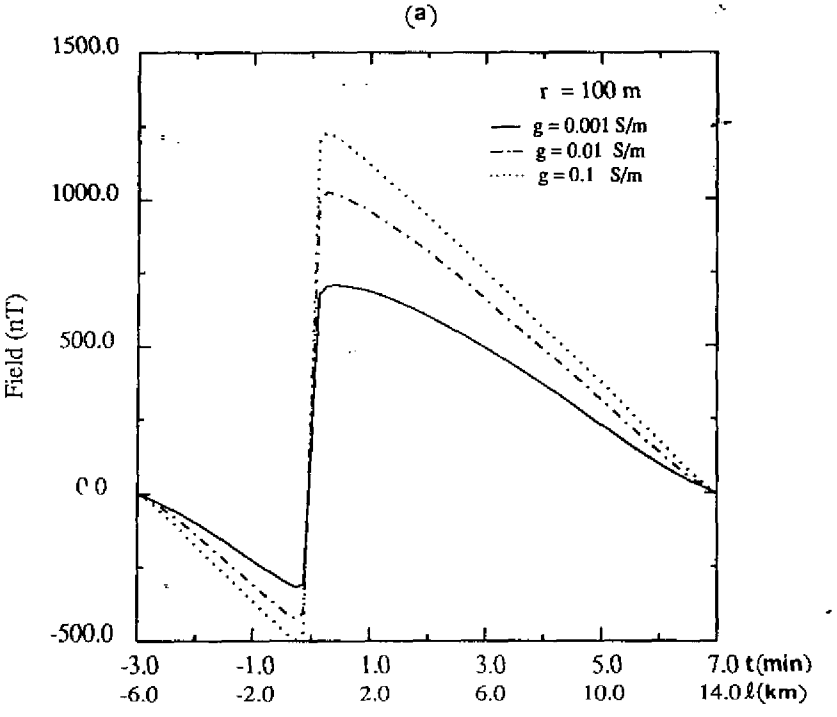
(a)
r = 100 m
g = 0.001 S/m
g = 0.01 S/m
g = 0.1 S/m
Field (nT)
1500.0
1000.0
500.0
0.0
-500.0
-3.0
-1.0
1.0
3.0
5.0
7.0 t(min)
-6.0
-2.0
2.0
6.0
10.0
14.0 ℓ(km)

Fig. 6a

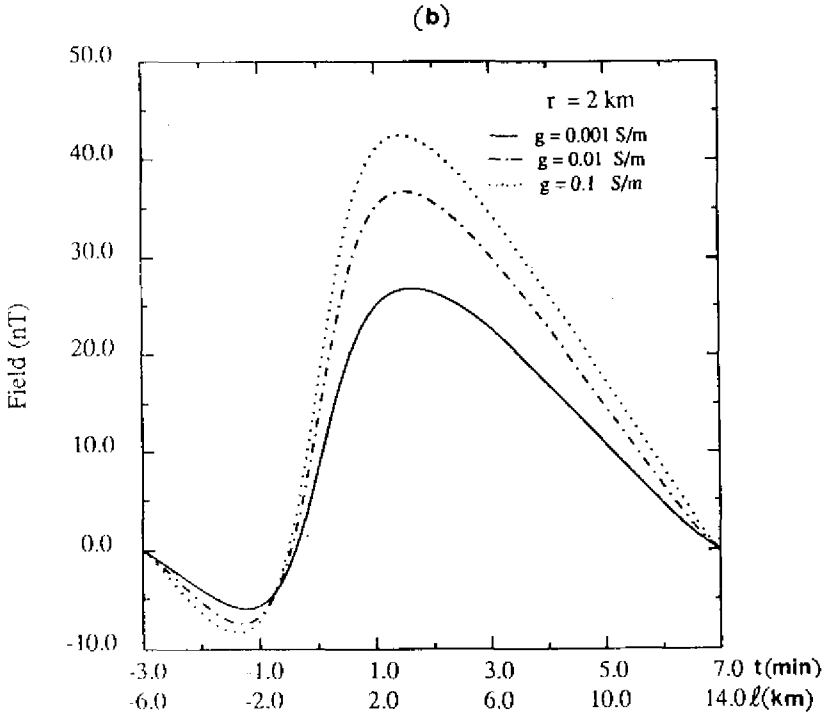
(b)
r = 2 km
g = 0.001 S/m
g = 0.01 S/m
g = 0.1 S/m
Field (nT)
50.0
40.0
30.0
20.0
10.0
0.0
-10.0
-3.0
-6.0
-1.0
-2.0
1.0
2.0
3.0
6.0
5.0
10.0
7.0 t(min)
14.0ℓ(km)

Fig.6b

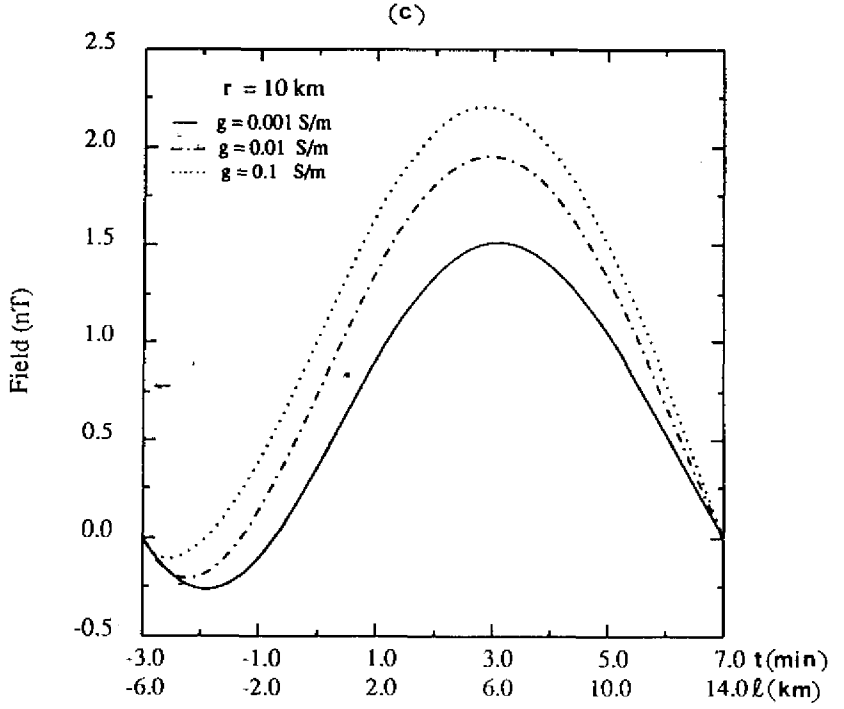
(c)
r = 10 km
g = 0.001 S/m
g = 0.01 S/m
g = 0.1 S/m
Field (nT)
2.5
2.0
1.5
1.0
0.5
0.0
-0.5
-3.0
-6.0
-1.0
-2.0
1.0
2.0
3.0
6.0
5.0
10.0
7.0 t(min)
14.0ℓ(km)

Fig.6c

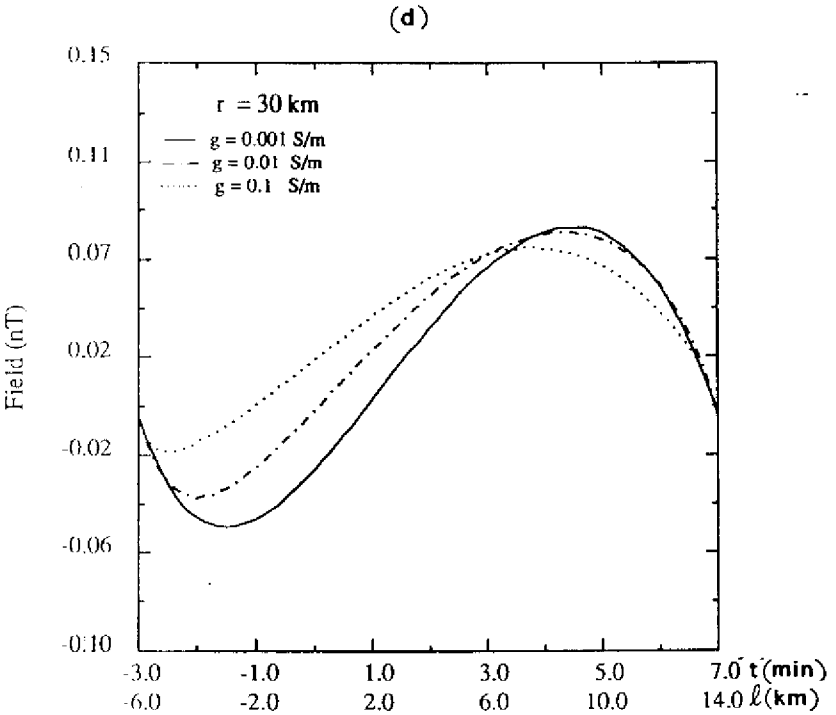
(d)
r = 30 km
g = 0.001 S/m
g = 0.01 S/m
g = 0.1 S/m
Field (nT)
0.15
0.11
0.07
0.02
-0.02
-0.06
-0.10
-3.0
-6.0
-1.0
-2.0
1.0
2.0
3.0
6.0
5.0
10.0
7.0 t(min)
14.0 ℓ(km)

Fig.6a

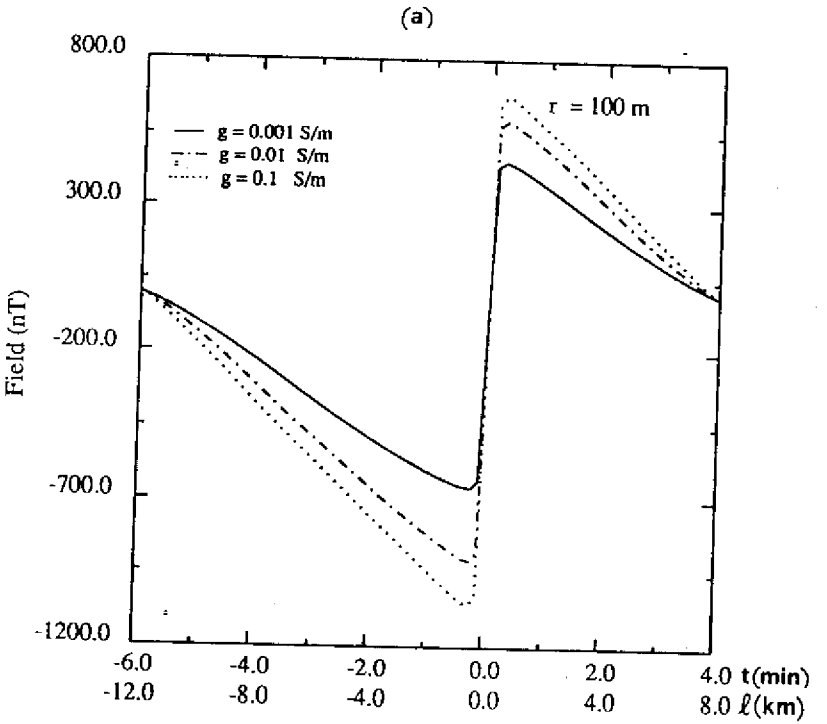
(a)
r = 100 m
g = 0.001 S/m
g = 0.01 S/m
g = 0.1 S/m
Field (nT)
800.0
300.0
-200.0
-700.0
-1200.0
-6.0
-12.0
-4.0
-8.0
-2.0
-4.0
0.0
0.0
2.0
4.0
4.0 t(min)
8.0 ℓ(km)

Fig.7a

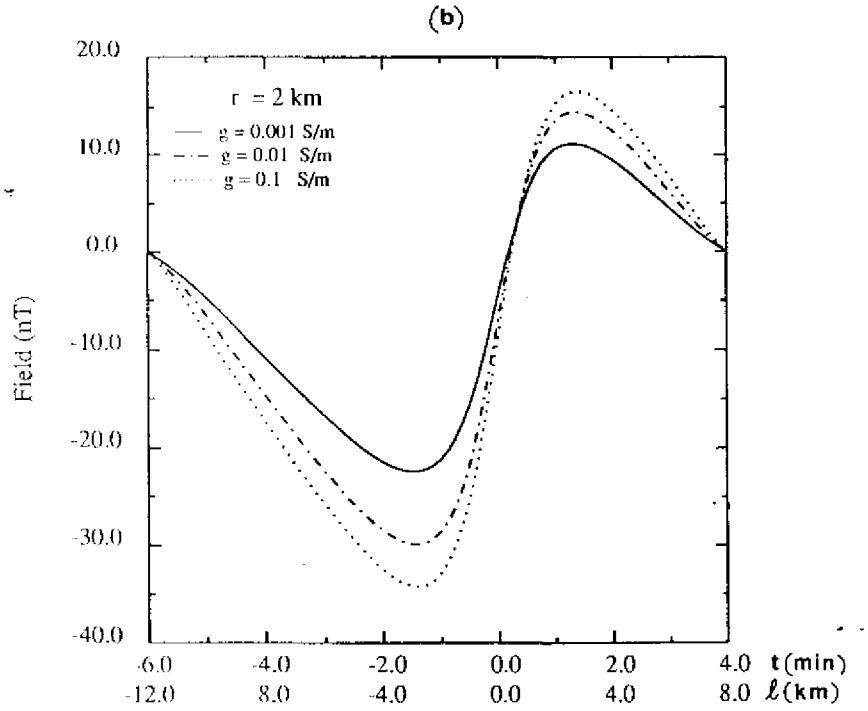
(b)
r = 2 km
g = 0.001 S/m
g = 0.01 S/m
g = 0.1 S/m
Field (nT)
20.0
10.0
0.0
-10.0
-20.0
-30.0
-40.0
-6.0
-12.0
-4.0
8.0
-2.0
-4.0
0.0
0.0
2.0
4.0
4.0
8.0
t(min)
ℓ(km)

Fig.7b

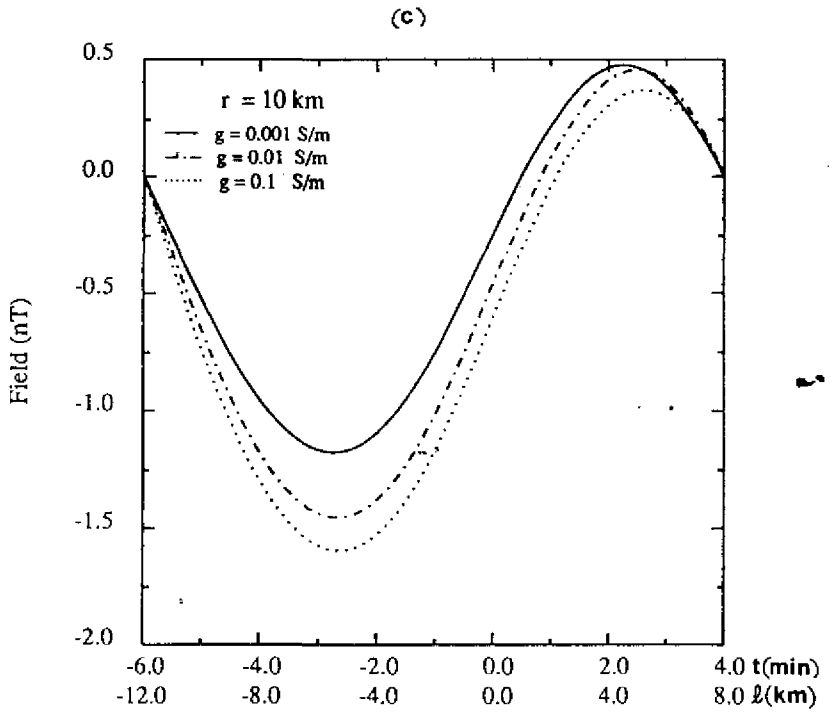
(c)
r = 10 km
g = 0.001 S/m
g = 0.01 S/m
g = 0.1 S/m
Field (nT)
0.5
0.0
-0.5
-1.0
-1.5
-2.0
-6.0
-12.0
-4.0
-8.0
-2.0
-4.0
0.0
0.0
2.0
4.0
4.0
8.0
t(min)
ℓ(km)

Fig.7c

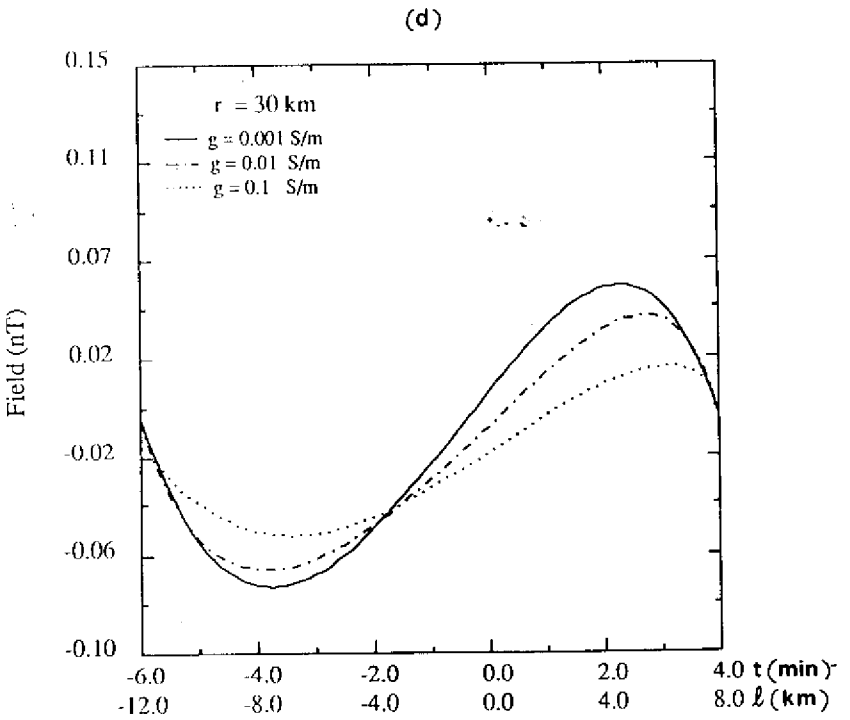
(d)
r = 30 km
g = 0.001 S/m
g = 0.01 S/m
g = 0.1 S/m
Field (nT)
0.15
0.11
0.07
0.02
-0.02
-0.06
-0.10
-6.0
-4.0
-2.0
0.0
2.0
4.0 t (min)
-12.0
-8.0
-4.0
0.0
4.0
8.0 ℓ (km)

Fig. 7a

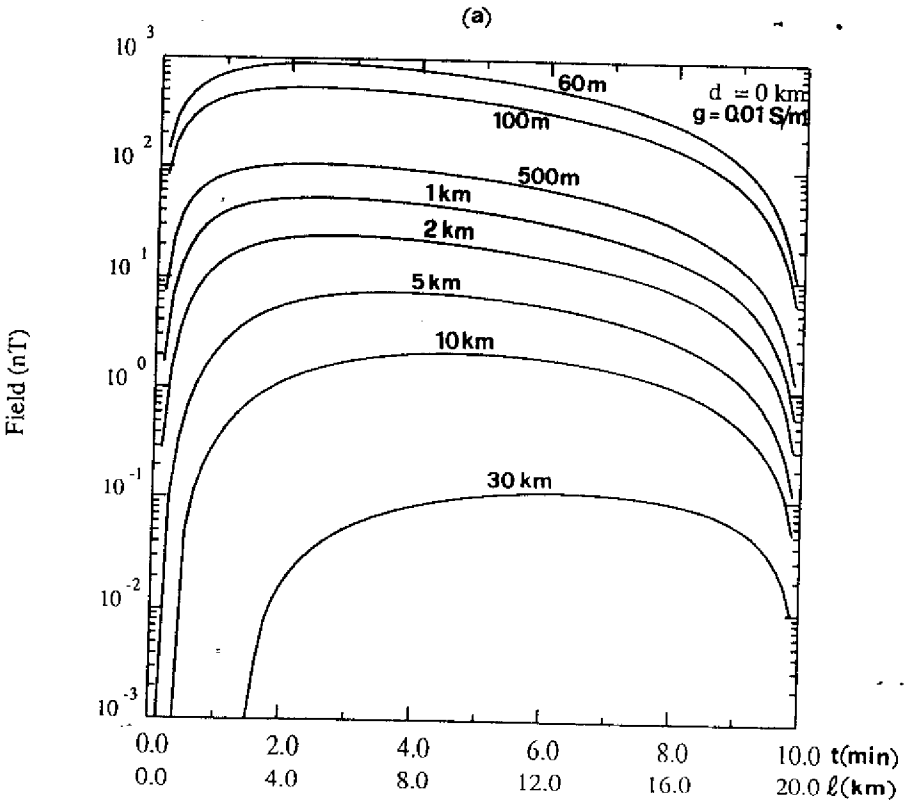
(a)
d = 0 km
g = 0.01 S/m
60m
100m
500m
1km
2km
5km
10km
30 km
Field (nT)
10 3
10 2
10 1
10 0
10 -1
10 -2
10 -3
0.0
2.0
4.0
6.0
8.0
10.0 t(min)
0.0
4.0
8.0
12.0
16.0
20.0 ℓ(km)

Fig. 8a

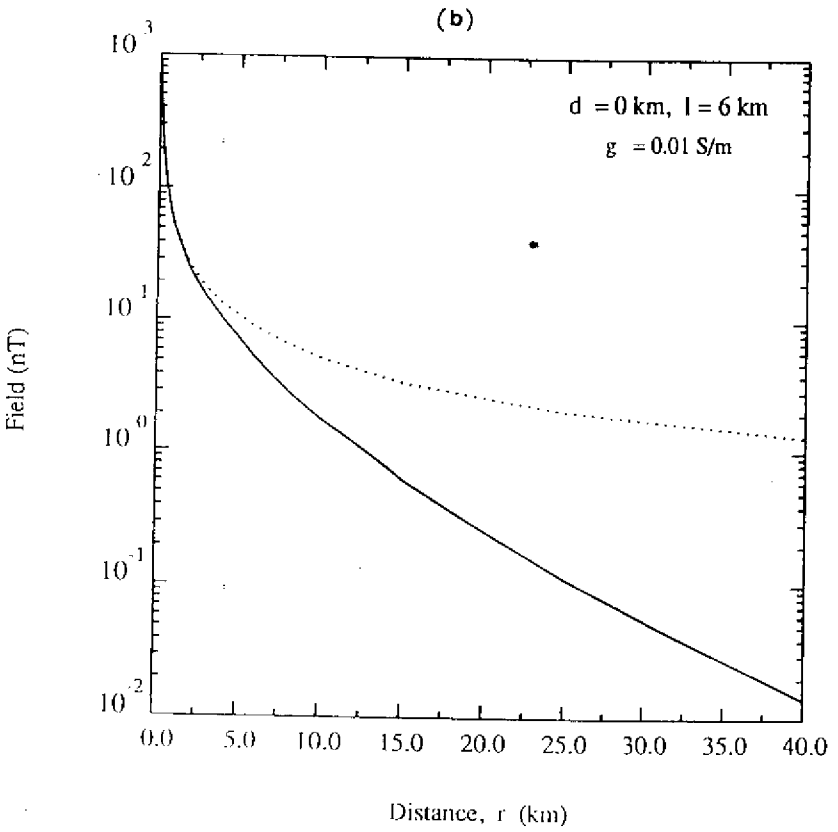
(b)
d = 0 km, l = 6 km
g = 0.01 S/m
Field (nT)
Distance, r (km)

Fig.8b

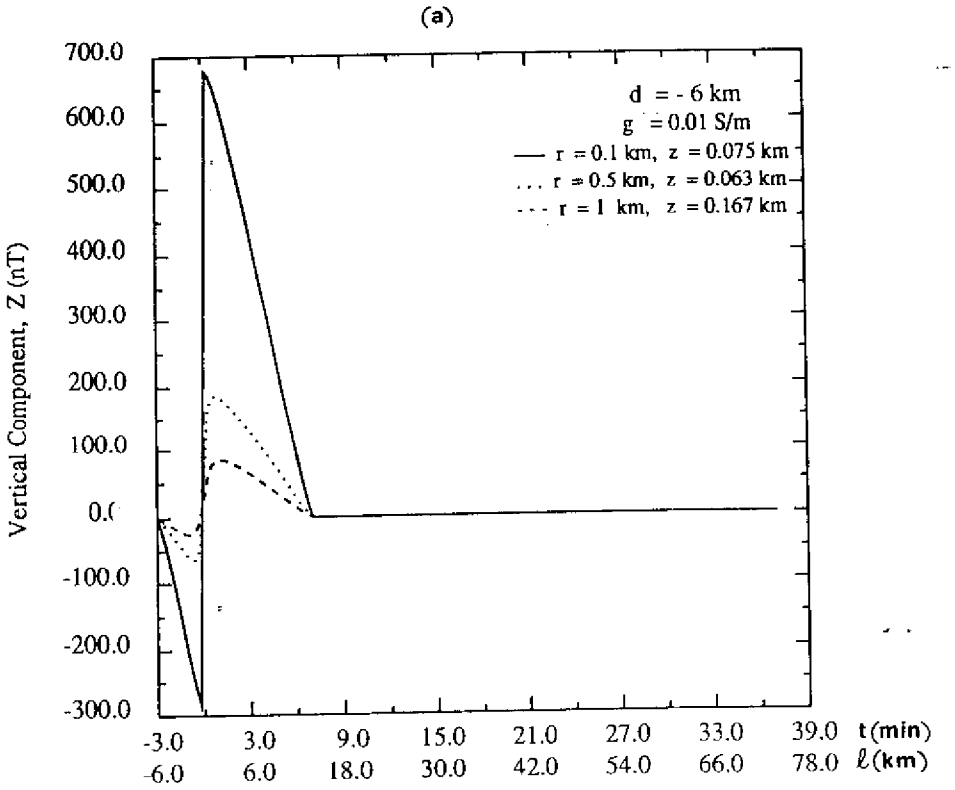
(a)
d = - 6 km
g = 0.01 S/m
r = 0.1 km, z = 0.075 km
r = 0.5 km, z = 0.063 km
r = 1 km, z = 0.167 km
Vertical Component, Z (nT)
t(min)
ℓ(km)

Fig.9a

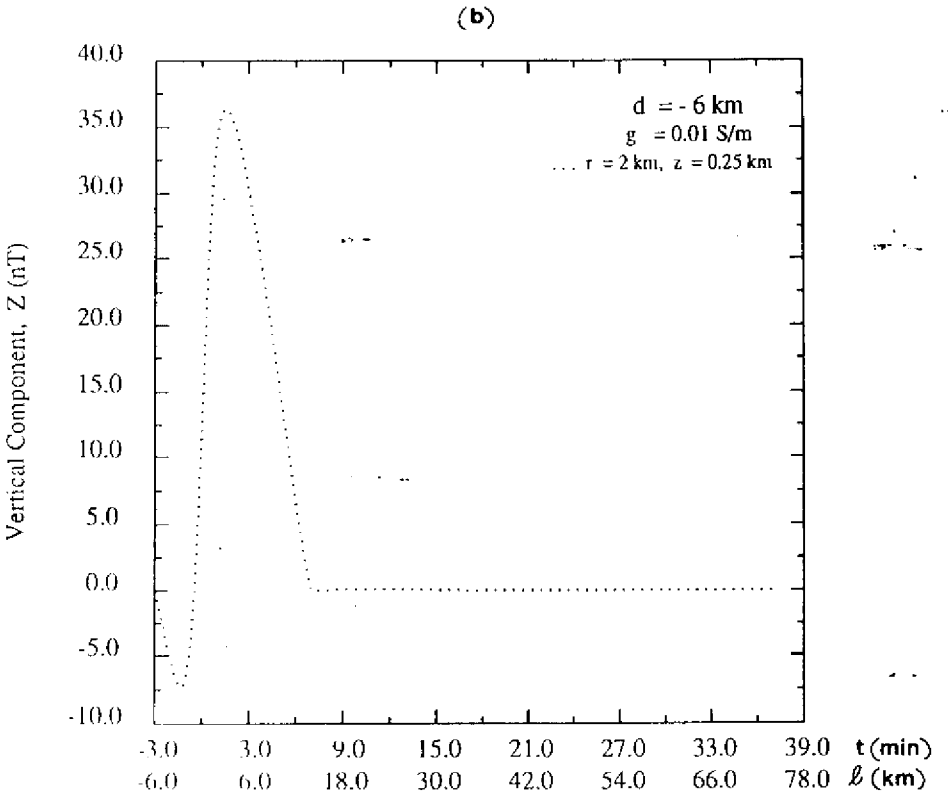
(b)
d = - 6 km
g = 0.01 S/m
... r = 2 km, z = 0.25 km
Vertical Component, Z (nT)
40.0
35.0
30.0
25.0
20.0
15.0
10.0
5.0
0.0
-5.0
-10.0
-3.0 3.0 9.0 15.0 21.0 27.0 33.0 39.0 t (min)
-6.0 6.0 18.0 30.0 42.0 54.0 66.0 78.0 ℓ (km)

Fig. 2b

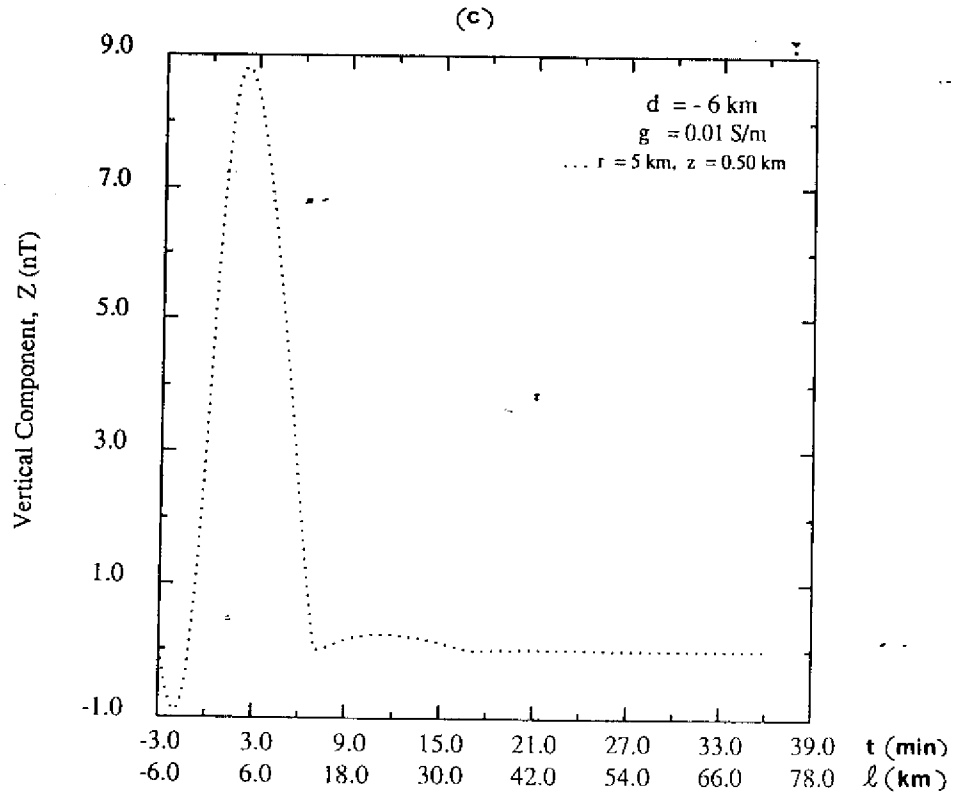
(c)
d = - 6 km
g = 0.01 S/m
... r = 5 km, z = 0.50 km
Vertical Component, Z (nT)
9.0
7.0
5.0
3.0
1.0
-1.0
-3.0 3.0 9.0 15.0 21.0 27.0 33.0 39.0 t (min)
-6.0 6.0 18.0 30.0 42.0 54.0 66.0 78.0 ℓ (km)

Fig. 2c

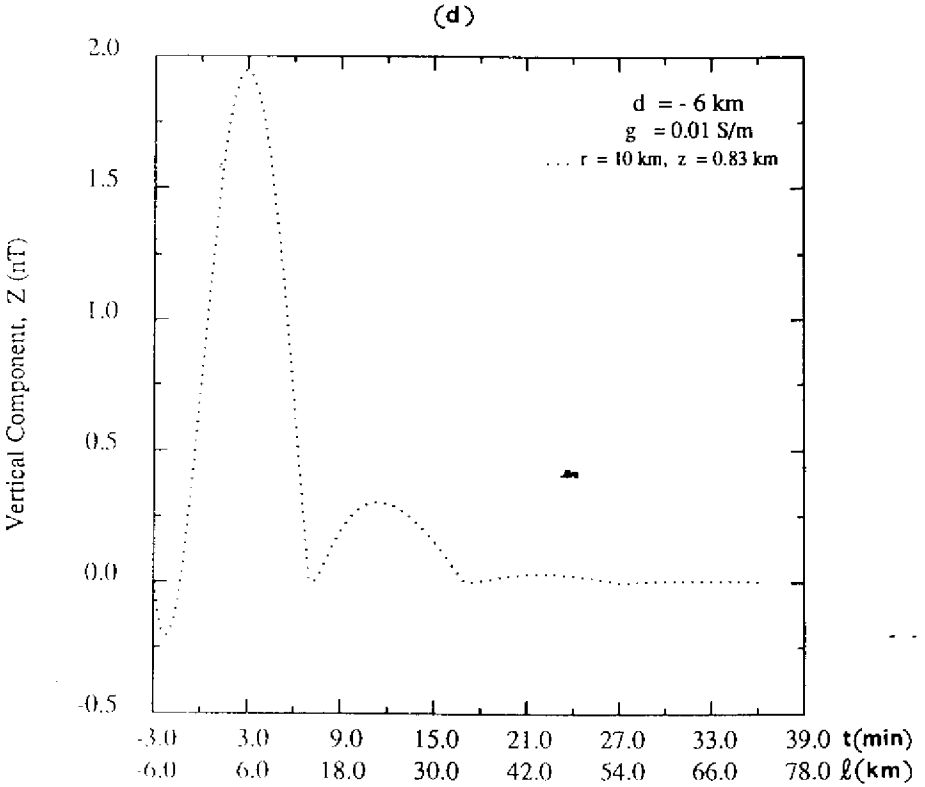
(d)
d = - 6 km
g = 0.01 S/m
... r = 10 km, z = 0.83 km
Vertical Component, Z (nT)
2.0
1.5
1.0
0.5
0.0
-0.5
-3.0
3.0
9.0
15.0
21.0
27.0
33.0
39.0 t(min)
-6.0
6.0
18.0
30.0
42.0
54.0
66.0
78.0 ℓ(km)

Fig.9

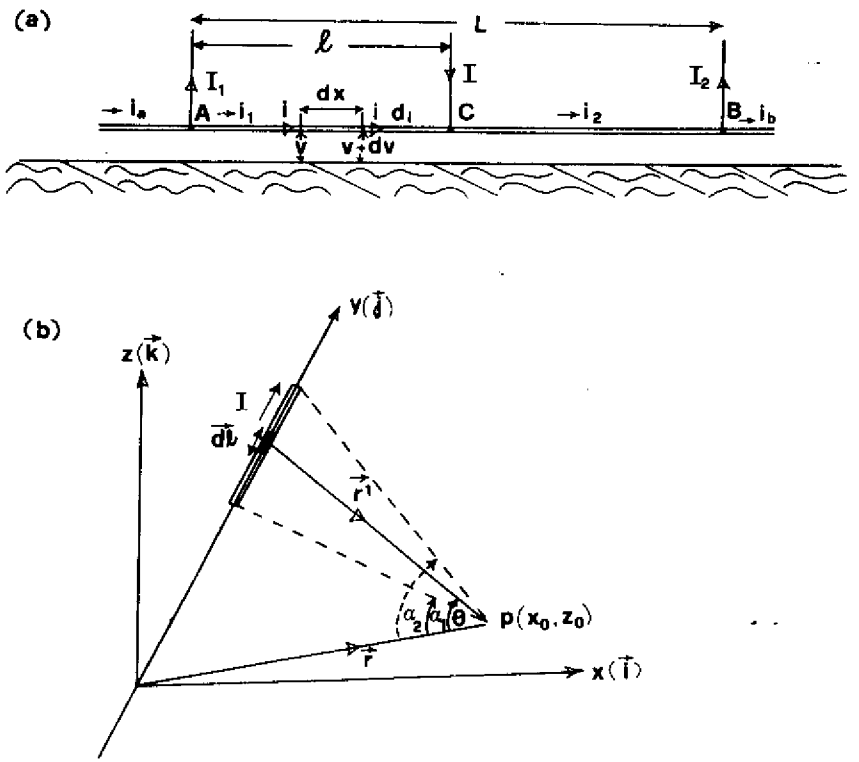
(a)
L
ℓ
I
I1
I2
dx
A
C
B
i1
i2
ia
ib
i
di
v
v+dv
(b)
y(j)
z(k)
I
dl
r1
r
p(x0, z0)
x(i)

Fig.10